Cancer Letters xxx (2016) 1–7

Contents lists available at ScienceDirect

Cancer Letters

journal homepage: www.elsevier.com/locate/canlet

Original Article

CRISPR-mediated targeting of *HER2* inhibits cell proliferation through a dominant negative mutation

Huajing Wang, William Sun*

Institute of Bioengineering and Nanotechnology, 31 Biopolis Way, #09-01 Nanos, Singapore 138669, Singapore

ARTICLE INFO

Article history:
Received 19 August 2016
Received in revised form
20 October 2016
Accepted 22 October 2016

Keywords:
Cas9
ERBB2
Breast cancer
PARP inhibitor
Trastuzumab
Therapeutic

ABSTRACT

With the discovery of the CRISPR/Cas9 technology, genome editing could be performed in a rapid, precise and effective manner. Its potential applications in functional interrogation of cancer-causing genes and cancer therapy have been extensively explored. In this study, we demonstrated the use of the CRISPR/Cas9 system to directly target the oncogene *HER2*. Directing Cas9 to exons of the *HER2* gene inhibited cell growth in breast cancer cell lines that harbor amplification of the *HER2* locus. The inhibitory effect was potentiated with the addition of PARP inhibitors. Unexpectedly, CRISPR-induced mutations did not significantly affect the level of HER2 protein expression. Instead, CRISPR targeting appeared to exert its effect through a dominant negative mutation. This HER2 mutant interfered with the MAPK/ERK axis of HER2 downstream signaling. Our work provides a novel mechanism underlying the anti-cancer effects of HER2-targeting by CRISPR/Cas9, which is distinct from the clinical drug Herceptin. In addition, it opens up the possibility that incomplete CRISPR targeting of certain oncogenes could still have therapeutic value by generation of dominant negative mutants.

Introduction

Cancer is a disease that stems from genetic alterations that includes point mutations, gene amplifications and translocations [1]. Most therapeutic approaches aim to target the phenotype of cancer, such as rapid cell division, a dysregulated signaling pathway, or an activated kinase that fuels growth. Unfortunately, most of these characteristics are shared by normal cells, thus resulting in undesirable side effects of chemotherapy. A therapeutic approach that directly targets the genomic changes could be valuable since it should, in principle, have no effect on wild type cells. Recent development of genome editing tools such as the clustered regularly interspaced short palindromic repeats (CRISPR) system could provide such an opportunity.

Type II CRISPR/CRISPR-associated protein nuclease (Cas9) system derived from *Streptococcus pyogenes* has been successfully employed for genome engineering in mammalian cells and animals [2–7]. In its most widely used form, CRISPR/Cas9 is composed of two components: the DNA endonuclease Cas9 and a chimeric single guide RNA (gRNA). The chimeric gRNA binds and recruits Cas9 to a specific genomic target sequence [8,9]. Specificity is conferred by the 20 nucleotides at the 5′ end of the gRNA that is complementary to the desired DNA sequence. In addition, a protospacer adjacent motif (PAM) located immediately downstream of the target sequence is essential for Cas9-mediated DNA cleavage at the target site. Cas9-induced double-stranded breaks (DBSs) can lead to error-prone repair by nonhomologous end-joining (NHEJ) [10], thereby enabling targeted disruption of specific genes.

In this study, we employed the CRISPR/Cas9 technology to target the *HER2* (*ERBB2*) gene in HER2-amplified breast cancer cells. *HER2* is a well-known oncogene and the therapeutic target for the monoclonal antibody Herceptin (trastuzumab). We showed that CRISPR/Cas9-mediated targeting of *HER2* inhibited cell proliferation and tumorigenicity. Furthermore, we demonstrated that the effect of CRISPR/Cas9 was markedly enhanced by the treatment of poly-ADP ribose polymerase (PARP) inhibitors. Surprisingly, CRISPR targeting of HER2 did not significantly reduce its protein expression level, though the downstream MAPK/ERK and PI3K/AKT signaling cascades were abrogated. These effects could partly be mediated by a dominant negative truncated form of HER2 generated through a frame-shift insertion in a *HER2* exon.

* Corresponding author.
E-mail address: wsun@ibn.a-star.edu.sg (W. Sun).

http://dx.doi.org/10.1016/j.canlet.2016.10.033
0304-3835/

Please cite this article in press as: H. Wang, W. Sun, CRISPR-mediated targeting of *HER2* inhibits cell proliferation through a dominant negative mutation, Cancer Letters (2016), http://dx.doi.org/10.1016/j.canlet.2016.10.033

Materials and methods

Molecular cloning of CRISPR/Cas9, HER2 and guide RNA design

To inactivate all isoforms of *HER2*, exons 5, 10 and 12 were chosen for targeting by single guide RNAs (gRNAs). Three pairs of gRNAs were designed using DNA2.0 gRNA Design Tool (https://www.dna20.com/eCommerce/cas9/input). The pCas9_GFP plasmid expressing *S. pyogenes* Cas9 was obtained from Addgene. Individual gRNAs were cloned into gRNA_Cloning vector (Addgene) according to the methodology online (http://www.addgene.org/41824/). *HER2*-specific gRNA sequences are as follow: exon5 (GTGCCAGTCCCGAGACCCAC), exon10 (GAGGGCCGGTATACATTCGG) and exon12 (GGGCATGGAGCACTTGCGAG). HER2 or gRNAs were cloned into pMX retroviral vector (Addgene), utilizing BamH1 and Not1 restriction sites via Gibson assembly. Wildtype HER2 cDNA clone (NM_004448.2) was purchased (Genecopoeia; EX-Z2866-M61) and single "C" insertion in *HER2* exon12 was generated using QuikChange II XL Site-Directed Mutagenesis Kit (Agilent Technologies).

Cell culture and drug treatments

Human breast cancer cell lines BT-474, SKBR-3 and MCF-7 were purchased from American Type Culture Collection (ATCC). BT-474, SKBR-3 and MCF-7 were maintained in RPMI (Gibco), McCoy's 5A (Modified) (Gibco) and 4500 mg/L glucose DMEM (Gibco) supplemented with 10% FBS (Gibco), 100 units/ml penicillin and 100 μg/ml streptomycin antibiotics (Gibco) at 37 °C with 5% CO_2, respectively. Human Embryonic Kidney (HEK) 293FT cells were cultured in DMEM under similar conditions. Cells were treated with Herceptin (10 μg/ml; a gift from Motoichi Kurisawa), SCR7 (10 μM; MedKoo), NU7441 (1 μM; Cayman Chemical), ME0328 (2 μM; Tocris Bioscience) and Veliparib (2 μM; Selleck Chemicals) for the indicated periods prior to functional assays.

Retrovirus production and transduction

pMX retroviral transfer vectors were co-transfected with VSV-G (Addgene) envelop plasmid into HEK293GP2 cells using FuGENE HD (Promega) or calcium phosphate (Clontech). Supernatants containing viral particles were harvested 24 h and 48 h post-transfection and were concentrated by Retro-Concentin according to the manufacturer's protocol (System Biosciences). For transduction, cells were incubated with virus-containing supernatants in the presence of 6 μg/ml polybrene (Sigma–Aldrich) for 8 h before replenishment with normal culture medium.

Transfection and cell proliferation assay

Breast cancer cell lines were transfected with Cas9 and gRNAs expression vectors using X-tremeGENE DNA transfection reagent according to the manufacturer's protocol (Roche). Briefly, cells were transfected or infected at 2×10^5 cells/well in 12-well plates for 3 days. They were then seeded in 96-well plates at 1×10^4 cells/well (BT-474 and SKBR-3) or 4000 cells/well (MCF7) for AlamarBlue cell proliferation assay. Fluorescence was measured at 530 nm and 590 nm wavelengths by Infinite M200 PRO plate reader (TECAN).

Soft agar colony formation assay

Transiently transfected cells were suspended in 0.4% agarose and culture media supplemented with 10% FBS and seeded over a basal layer of 0.6% agarose. The experiments were set up in 6-well plates at 1×10^5 cells/well in triplicates. Images from 6 different fields were captured for each biological replicate. The number of colonies ≥50 μm in size was scored 1–3 weeks after culture at 37 °C.

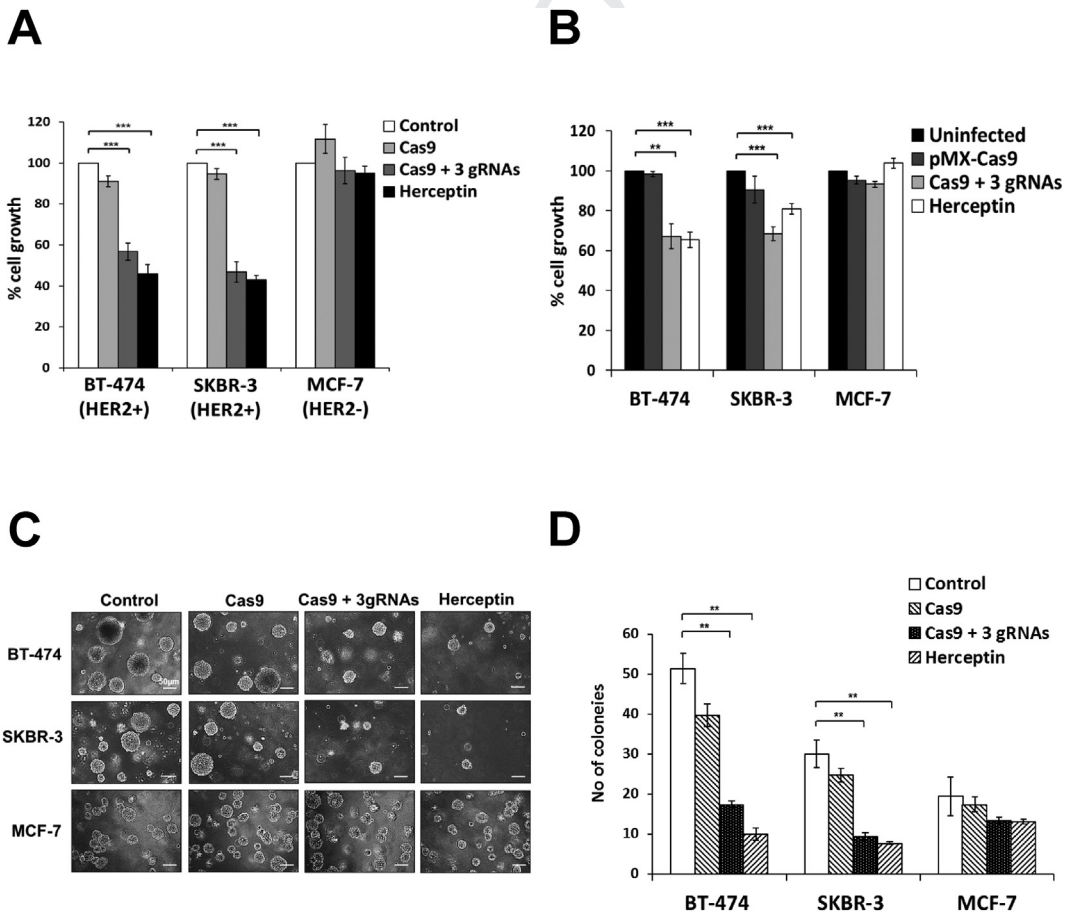

Fig. 1. Targeting of *HER2* by CRISPR/Cas9 reduced cell growth and tumorigenicity. (A) HER2-positive breast cancer cell lines BT-474 and SKBR-3 and HER2−negative MCF-7 cells were transfected with plasmids expressing Cas9 alone or together with 3 gRNAs that target exons 5, 10 and 12 of *HER2*. Cell proliferation was evaluated by AlamarBlue assay 6 days post-transfection. Cells treated with Herceptin at 10 μg/ml for 6 days served as positive control. Three independent experiments consisting of technical duplicates were performed. The values were plotted relative to the untransfected control sample for each cell line (means ± SEM, n = 6). (B) Breast cancer cells were transduced with pMX-based retroviruses encoding Cas9 alone or in combination with *HER2*-targeting 3gRNAs or subjected to Herceptin treatment (10 μg/ml) for 6 days prior to AlamarBlue assay. The data was normalized to the uninfected control sample (means ± SEM, n = 6). (C) The tumorigenic potential was assessed by soft agar colony-forming assay. Representative phase contrast images are shown. Scare bar = 50 μm. (D) The number of colonies ≥50 μm in size were scored 1–3 weeks after plating (means ± SEM, n = 3). Double and triple asterisks represent *p* value < 0.01 and < 0.001, respectively.

Please cite this article in press as: H. Wang, W. Sun, CRISPR-mediated targeting of *HER2* inhibits cell proliferation through a dominant negative mutation, Cancer Letters (2016), http://dx.doi.org/10.1016/j.canlet.2016.10.033

A

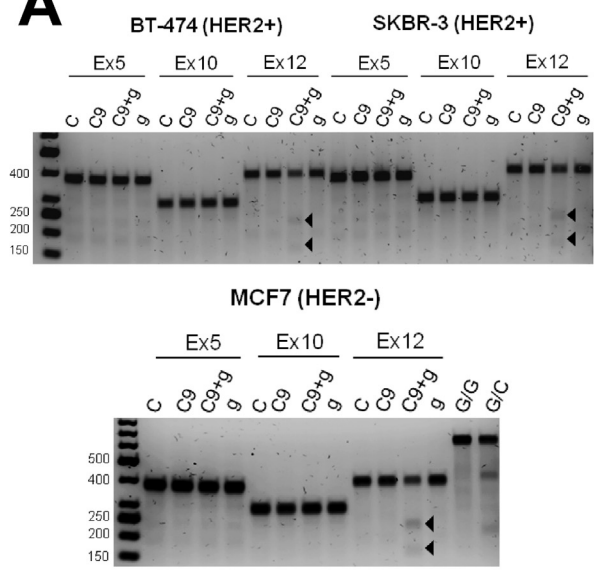

B

Human *HER2* exon12

5'…GCTATGGTCTGGGCATGGAGCACTTGCGAGAGGTGAGGGCAGT…3'

PAM

Cell line	Mutation frequency
BT-474	9.1% (4/44)
SKBR-3	9.1% (4/44)
MCF-7	24.4% (10/41)

C

Indels in human *HER2* exon12 locus

PAM

```
WT   GGTCTGGGCATGGAGCACTTGC---GAGAGGTGAGG
+1   GGTCTGGGCATGGAGCACTTGCC--GAGAGGTGAGG  (83.2%, 15/18)
+3   GGTCTGGGCATGGAGCACTTGCAGCGAGAGGTGAGG  (5.6%, 1/18)
D2   GGTCTGGGCATGGAGCACTTG-----GAGAGGTGAGG  (5.6%, 1/18)
D4   GGTCTGGGCATGGAGCAC---------AGAGGTGAGG  (5.6%, 1/18)
```

D

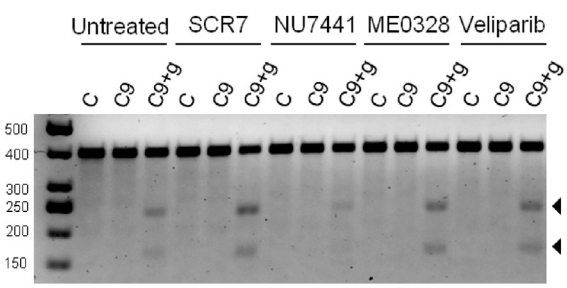

E

Samples	Mutation frequency
Untreated	15.5% (7/45)
SCR-7	31.8% (14/44)
ME0328	45.5% (20/44)
Veliparib	30% (12/40)

Indels in human *HER2* exon12 locus

PAM

```
WT   GGTCTGGGCATGGAGCACTTGC--GAGAGGTGAGG
+1   GGTCTGGGCATGGAGCACTTGCCGAGAGGTGAGG  (86.8%, 46/53)
+1D3 GGTCTGGGCATGGAGCACT---CGAGAGGTGAGG  (1.9%, 1/53)
+1D5 GGTCTGGGCATGGAGCACTTGCC-----GTGAGG  (1.9%, 1/53)
+1   GGTCTGGGCATGGAGCACTTGCAGAGAGGTGAGG  (1.9%, 1/53)
D2   GGTCTGGGCATGGAGCACTTGC---GAGGTGAGG  (3.8%, 2/53)
D4   GGTCTGGGCATGGAGCAC-----GAGAGGTGAGG  (1.9%, 1/53)
D6   GGTCTGGGCATGGAGC-------GAGAGGTGAGG  (1.9%, 1/53)
```

F

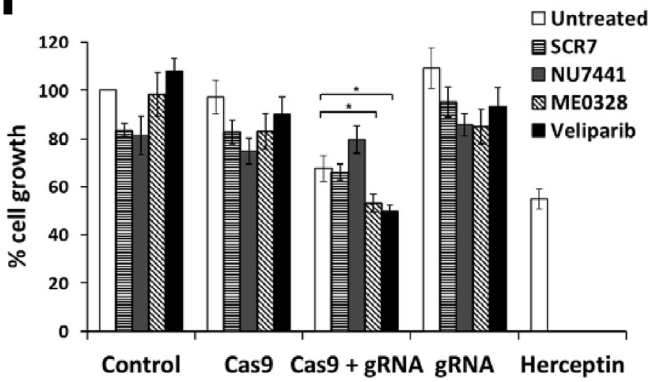

Please cite this article in press as: H. Wang, W. Sun, CRISPR-mediated targeting of *HER2* inhibits cell proliferation through a dominant negative mutation, Cancer Letters (2016), http://dx.doi.org/10.1016/j.canlet.2016.10.033

T7 endonuclease I assay and mutation analysis

Genomic DNA was extracted by DNeasy blood and tissue kit (Qiagen) according to manufacturer's protocol and *HER2* exons were amplified by PCR. PCR products were denatured and reannealed with the following steps: 95 °C for 10 min, 95 °C–85 °C with ramping at 2 °C/s, 85 °C–25 °C with ramping at 0.1 °C/s, hold at 25 °C for 1 min. Reannealed PCR products were digested with T7 endonuclease I (New England Biolabs) for 30 min at 37 °C. To characterize Cas9-induced mutations, A-overhangs were added to PCR amplicons using *Taq* DNA polymerase (New England Biolabs) before cloning into the pCR2.1 vector via TOPO TA cloning kit (Invitrogen). Sequences of individual clones were verified by Sanger sequencing. PCR primer sequences are shown in Supplementary Table S1.

Western blot analysis

Cell pellets were lysed by RIPA buffer (Pierce) and whole cell lysates were subjected to electrophoresis on 4–15% SDS-polyacrylamide gels (Bio-Rad). Immunoblotting was performed with antibodies against human HER2: Ab2428 (1:1000 dilution; Abcam) and M45 (1:1000 dilution; Cell Signaling), phospho-HER2^{Y1248} (1:2000 dilution; Santa Cruz), phospho-HER2^{Y1221} (1:1000 dilution; Cell Signaling), ERK (1:1000 dilution; Santa Cruz), phospho-ERK$^{Y202/204}$ (1:1000 dilution; Santa Cruz), AKT (1:1000 dilution; Cell Signaling), phospho AKT^{S473} (1:1000 dilution; Cell Signaling), Cas9 (1:1000 dilution; Active Motif), α-tubulin (1:10000 dilution; Sigma–Aldrich) and β actin (1:2500 dilution; Santa Cruz). Immunoblots were quantified using ImageJ software in which protein band intensities were measured in technical triplicates.

Flow cytometry analysis

MCF-7 cells were transfected with HER2 expression vectors and analyzed on FACS Calibur (BD Biosciences, USA) based on GFP fluorescence. Cells were stained with Allophycocyanin (APC)-conjugated antibody against HER2 receptor (1:200 Biolegend) and APC-mouse IgG1 κ was used as isotype control (Biolegend).

Statistical analysis

All data were presented as mean ± SEM. One-way Analysis of Variance (*ANOVA*) and Tukey's Post Hoc tests were performed where p value of <0.05 was considered significant.

Results

Targeting of HER2 by CRISPR/Cas9 inhibited cell proliferation and tumorigenicity in breast cancer cells

We designed gRNAs to selectively target *HER2* exons 5, 10 and 12 in an attempt to disrupt its function. These exons are present in all isoforms of HER2 and encode parts of the extracellular domain, and thus, targeting of these exons would likely lead to functional gene disruption. Three gRNAs were introduced together with Cas9 into HER2-positive (BT-474, SKBR-3) and HER2–negative (MCF-7) breast cancer cell lines by transient transfection. As shown in Fig. 1A, co-expression of Cas9 and 3 gRNAs significantly reduced cell growth, and this effect was observed in BT-474 and SKBR-3 but not in MCF-7 cells. The magnitude of growth inhibition was comparable to that of Herceptin treatment, a clinical drug used for treating HER2-positive breast cancers. Overexpression of Cas9 alone did not affect cell growth, indicating the absolute requirement of gRNAs for *HER2* targeting (Fig. 1A). To verify the above observations, the same panel of breast cancer cell lines were transduced with retroviruses encoding Cas9 alone or together with *HER2*-specific gRNAs. Similar to the result with transient transfection, cells transduced with the Cas9/3gRNAs combination displayed significant reduction in cell proliferation, and the effect was limited to the HER2-positive cell lines (Fig. 1B). We also examined the effect of Cas9/3gRNAs in the soft agar colony formation assay, an indicator of tumorigenicity *in vitro*. Consistent with the reduction in cell proliferation, a significant decrease in colony formation was observed (Fig. 1C and D). Together, these results indicated that CRISPR/Cas9-mediated *HER2* targeting suppressed cell growth and tumorigenicity in HER2-positive breast cancer cells, but not in a HER2-negative cell line.

CRISPR/Cas9 induced mutations in HER2 and its targeting is enhanced by PARP inhibitors

To confirm CRISPR/Cas9-induced mutagenesis in the transfected cells, genomic fragments in the targeted *HER2* exons were PCR amplified and assayed by T7 endonuclease I to detect mismatched DNA. As shown in Fig. 2A, DNA cleavage fragments were produced exclusively from *HER2* exon12 in cells overexpressing Cas9/3gRNAs. The extent of mismatch cleavage was surprisingly low, and undetectable in exons 5 and 10. To characterize the mutations, PCR amplicons encompassing *HER2* exon12 were cloned and individual clones were analyzed by Sanger sequencing. All mutations found were located at the predicted Cas9 cleavage site upstream of the PAM motif (Fig. 2B). In BT-474 or SKBR-3 cells, 4 out of 44 reads (9.1%) contained indel mutations. In contrast, 10 out of 41 (24.4%) sequencing reads from MCF-7 cells contained mutations (Fig. 2B). Interestingly, the majority (83.2%) of mutations was a single "C" nucleotide insertion (Fig. 2C).

To rule out possible off-target effect of the gRNA designed for *HER2* exon12, we performed a BLAST search against the human genome and transcripts. The result showed that the nearest matches have up to 75% identity with our gRNA and were found within the transcripts of three genes – *RNF219*, *SH3BP5L* and *CNN* (Fig. S1A and S1B). We PCR amplified these regions after treating the cells with Cas9/gRNA and subjected them to the T7 endonuclease I assay. The results showed that Cas9/gRNA induced DNA cleavage specifically in *HER2* exon12, but not in the fragments amplified from *RNF219*, *SH3BP5L*, and *CNN1* (Fig. S1C). This observation was consistent across three breast cancer cell lines BT-474, SKBR-3 and MCF-7. Therefore, guide RNA targeting *HER2* exon12 appeared to be highly specific and did not show off-target DNA cleavage in the three genes tested.

Because the frequency of CRISPR induced mutations in *HER2* exon12 was low, we attempted to increase the mutational rate by enhancing error-prone repair. It has been reported that inhibition of DNA repair pathways sensitized cancer cells to

Fig. 2. *HER2*-specific gRNA/Cas9 induced mutations and PARP inhibitors enhanced its targeting efficiency. (A) Cas9 and 3 gRNAs targeting *HER2* exons 5, 10 and 12 expression vectors were co-transfected into BT-474, SKBR-3 and MCF-7 breast cancer cell lines. This was followed by PCR amplification of the respective exons of *HER2* from genomic DNA. T7 endonuclease I assay was employed to detect mutations induced by Cas9. The predicted sizes of DNA cleavage products for *HER2* exon12 are 160 bp and 234 bp as indicated by the arrows. The DNA ladder is shown on the first lanes (top and bottom panels). DNA homoduplexes G/G and its heteroduplex counterpart G/C containing a "C" point mutation served as negative and positive controls, respectively (bottom panel). C: Control; C9: Cas9; C9+g: Cas9+ 3gRNAs targeting exons 5, 10 and 10 of *HER2*; Ex5: exon5; Ex10: exon10; Ex12: exon12. (B) PCR products containing *HER2* exon12 were cloned and individual clones were sequenced. The *HER2* exon12-specific gRNA sequence is underlined. Red arrow: Cas9 cutting site. (C) Summary of the various types of indel mutations induced by CRISPR/Cas9. Red letters: insertions; red dashes: deletions. WT: wildtype; +: insertion; D: deletion. (D) HER2-positive breast cancer cells BT-474 were co-transfected with Cas9 and single gRNA targeting *HER2* exon12 and concurrently treated with SCR7 (DNA ligase IV inhibitor; 10 μM), NU7441 (DNA-PKs inhibitor; 1 μM), ME0328 (PARP3 inhibitor; 2 μM), or Veliparib (PARP1/2 inhibitor; 1 μM) for 3 days. The cells were harvested for genomic DNA extraction and subjected to T7 endonuclease I assay to detect mutations. C: Control; C9: Cas9; C9+g: Cas9+ single gRNA targeting *HER2* exon12. (E) Mutation frequencies with various inhibitor treatments are shown in the table (top panel). Different types of indel mutations induced by CRISPR/Cas9 are summarized (bottom panel). Red arrow: Cas9 cleavage site; red letters: insertions; red dashes: deletions. WT: wildtype; +: insertion; D: deletion. (F) BT-474 cells were transfected and simultaneously treated with various DNA repair inhibitors SCR7, NU7441, ME0328 or Veliparib. Cell proliferation was ascertained by AlamarBlue assay 6 days post transfection. Three biological experiments with technical duplicates were performed. The values are expressed relative to the untransfected/untreated control (means ± SEM, n = 6). One asterisk denotes p value < 0.05. (For interpretation of the references to color in this figure legend, the reader is referred to the web version of this article.)

Please cite this article in press as: H. Wang, W. Sun, CRISPR-mediated targeting of *HER2* inhibits cell proliferation through a dominant negative mutation, Cancer Letters (2016), http://dx.doi.org/10.1016/j.canlet.2016.10.033

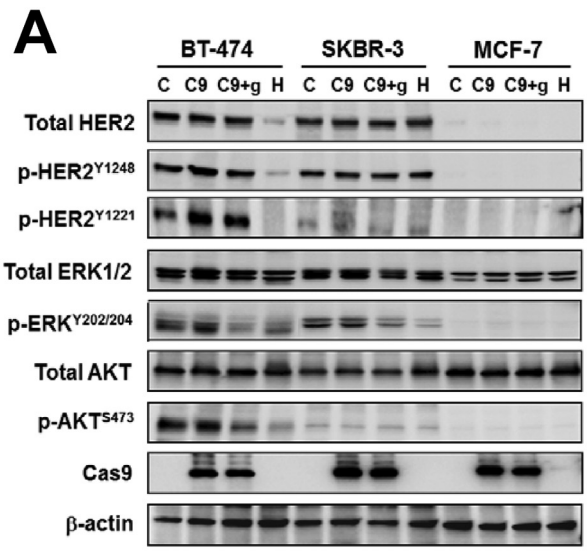

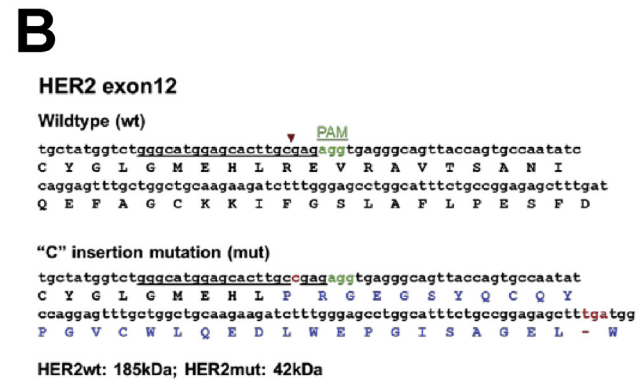

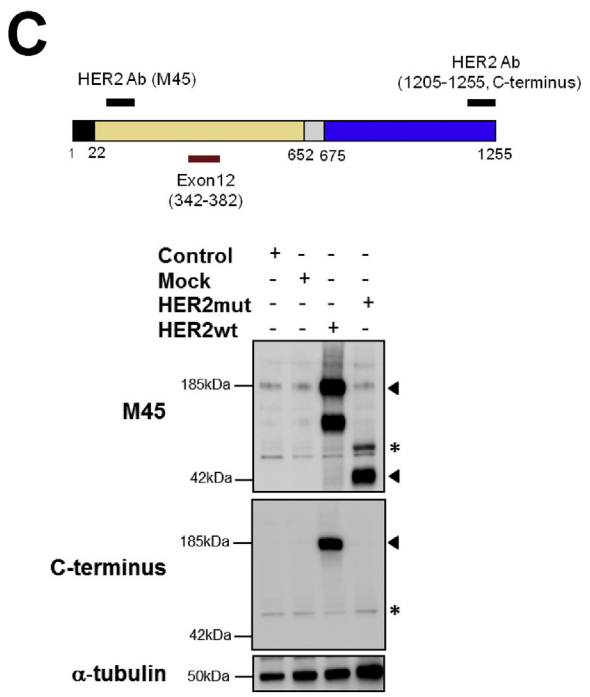

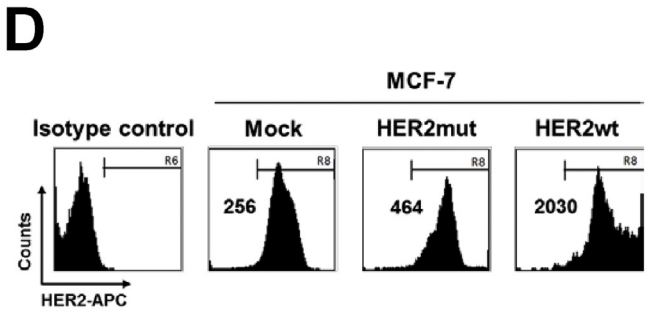

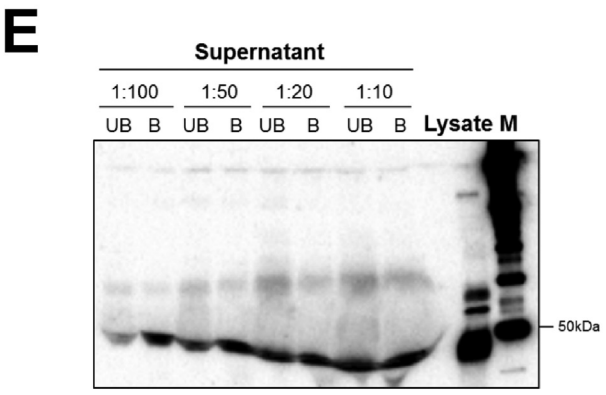

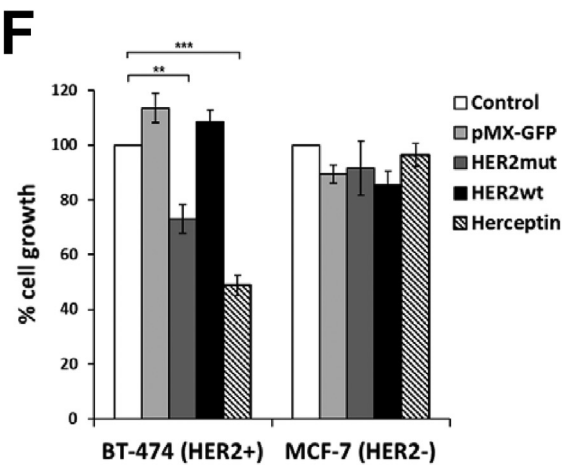

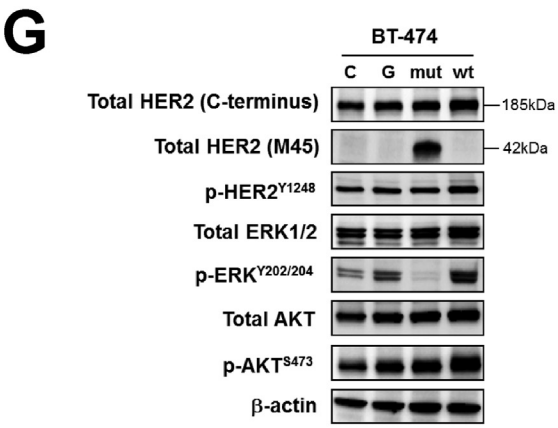

Please cite this article in press as: H. Wang, W. Sun, CRISPR-mediated targeting of *HER2* inhibits cell proliferation through a dominant negative mutation, Cancer Letters (2016), http://dx.doi.org/10.1016/j.canlet.2016.10.033

chemotherapeutic drugs that generate DBSs [11]. We therefore tested the effect of DNA repair inhibitors on CRISPR/Cas9 activity in our system. SCR7 is an inhibitor of DNA ligase IV while NU7441 is a selective inhibitor of DNA-dependent protein kinases (DNA-PKs), both targeting the non-homologous end joining (NHEJ) DNA repair pathway [12,13]. Veliparib (ABT-888) and ME0328 are selective inhibitors of PARP1/2 and PARP3, respectively [14,15]. HER2-positive breast cancer cells BT474 were co-transfected with Cas9 and a single gRNA targeting *HER2* exon12 and concurrently treated with various DNA repair inhibitors. Our results showed that treatment with SCR7, ME0328, or Veliparib enhanced CRISPR/Cas9-induced mutagenesis (Fig. 2D). Treatment with NU-7441 did not appear to increase the mutation frequency. In this experiment, while the basal mutation rate was 15.5%, the mutation frequency was increased significantly in the presence of SCR7 (31.8%), ME0328 (45.4%), or Veliparib (30%) (Fig. 2E). Consistently, a single "C" nucleotide insertion was the major mutation product (Fig. 2E). Functionally, treatment with ME0328 or Veliparib augmented the anti-proliferative activity of CRISPR/Cas9 while there was no effect on their own (Fig. 2F). Therefore, these results indicated that PARP inhibitors can enhance CRISPR/Cas9-mediated *HER2* targeting, leading to a greater level of cell growth inhibition.

Frame-shift mutation in HER2 exon12 generated a dominant negative mutant

To understand the mechanistic action of CRISPR/Cas9 on HER2 signaling pathway, we analyzed the phosphorylation status of HER2, ERK 1/2 and AKT by Western blotting using phospho-specific antibodies. A clear down-regulation of p-ERK$^{Y202/204}$ was observed in the presence of Cas9/3gRNAs in HER2-positive BT-474 and SKBR-3 cell lines. Moreover, the reduction in p-AKT^{S473} was apparent in BT-474 but not in SKBR3 cells due to its low basal level. Surprisingly, there was no change in both the total HER2 protein level and phosphorylation at its two major autophosphorylation sites, Y1248 and Y1221 (Fig. 3A). In contrast, Herceptin treatment caused a marked reduction in total HER2, p-HER2^{Y1248}, p-HER2^{Y1221}, p-ERK$^{Y202/204}$ and p-AKT^{S473} in BT-474 cells (Fig. 3A). The blots were quantified using Image J software and the graphical results are shown in Fig. S2A. Collectively, these results indicated that CRISPR/Cas9 inhibited the HER2 downstream signaling pathways through a mechanism distinct from that of Herceptin.

Because CRISPR/Cas9 induced a predominant single "C" nucleotide insertion in *HER2* exon12 (Fig. 2C and E), we further characterized the functional effect of this mutation. As shown in Fig. 3B, insertion of a "C" at the Cas9 cutting site would result in a frame-shift and produce a truncated protein (HER2mut) with a molecular weight of 42 kDa instead of the 185 kDa wildtype (HER2wt) (Fig. 3B). To confirm this, two different antibodies recognizing either the extracellular domain (M45) or intracellular C-terminus (Ab2428) of HER2 were used to analyze HER2wt and HER2mut proteins overexpressed in 293FT cells by Western blotting. Our results showed that both HER2mut and HER2wt were detected by the M45 antibody at their predicted sizes of 42 kDa and 185 kDa, respectively. However, only HER2wt but not HER2mut was detected by the C-terminus antibody (Fig. 3C). When overexpressed in HER2-negative MCF-7 cells, HER2wt induced a 10-fold increase in HER2 expression on the cell surface while HER2mut did not cause any significant increase (Fig. 3D). In addition, HER2mut protein could be detected in the cell culture supernatant (Fig. 3E).

To functionally assay the effect of HER2mut on cell proliferation, retroviruses encoding HER2mut or HER2wt were transduced into BT-474 and MCF-7 cells. Cell growth was significantly suppressed upon the overexpression of HER2mut but not HER2wt. This growth inhibitory effect was restricted to BT-474 cells (Fig. 3F). With regards to HER2 signaling, the protein expression of p-ERK$^{Y202/204}$ was markedly reduced in the presence of HER2mut, but there was no change in p-AKT^{S473} (Fig. 3G and Fig. S2B). Total HER2 expression levels and its phosphorylation at Y1248 remained unchanged (Fig. 3G and Fig. S2B). Together, these results indicated that CRISPR targeting of *HER2* exon12 in HER2-positive cells produced a dominant negative mutant which inhibited cell proliferation and HER2 signaling.

Discussion

In this study, we utilize the CRISPR/Cas9 system to selectively target the *HER2 (ERBB2)* gene in human breast cancer cell lines harboring *HER2* amplification. We showed that ectopic expression of Cas9/3gRNAs against *HER2* exons profoundly suppressed cell proliferation and tumorigenicty in HER2-positive cell lines. Genomics analysis confirmed that CRISPR/Cas9 induced mutations in *HER2* exon12 which could disrupt gene function. However, the mutation frequencies were surprisingly low despite the strong phenotypic effects.

An interesting finding was the predominant single "C" nucleotide insertion in *HER2* exon12 induced by CRISPR/Cas9. Such a frame-shift mutation produced a truncated HER2mut protein that showed a dominant negative effect in suppressing cell proliferation. Growth inhibition was accompanied by a downregulation of the endogenous MAPK-ERK but not PI3K/AKT signaling in HER2-amplified cells. Unexpectedly, CRISPR/Cas9 or HER2mut did not cause a direct downregulation of HER2 protein expression and its autophosphorylations. Thus, the anti-tumorigenic effect of CRISPR/

Fig. 3. Mutation in *HER2* exon12 generated a truncated protein with dominant negative function. (A) Changes in protein expression were determined by Western blotting 3. days post-transfection. Total HER2 expression level was measured by a HER2-specific antibody that recognized the C-terminus of HER2 (Abcam). Phosphorylation of HER2, ERK1/2, and AKT was detected by phospho−specific antibodies. Immunodetection of β-actin served as loading control. C: Control; C9: Cas9; C9+g: Cas9+ 3gRNAs targeting exons 5, 10 and 12 of *HER2*; H: Herceptin. (B) A diagram depicting the DNA and amino acid sequences of HER2 exon12. Red arrow: Cas9 cleavage site; blue: altered amino acid sequences; red: "C" insertion mutation and stop codon. (C) A schematic diagram showing the HER2 protein. Black bars: epitopes for 2 separate anti-HER2 antibodies; red bar: HER2 exon12. Amino acids 1–22: signal peptide; 23–652: extracellular domain; 653–675: transmembrane domain; 676–1255: intracellular C-terminus. Wildtype HER2 (HER2wt) or HER2 bearing "C" insertion in exon12 (HER2mut) were transfected into 293FT cells and Western blotting was performed 2 days post-transfection. Exogenous HER2 proteins were detected using 2 different anti-HER2 antibodies M45 and C-terminus. Asterisk denotes unspecific bands. The signal for α-tubulin served as loading control. (D) HER2 negative MCF-7 cells were transfected with HER2wt or HER2mut expression vectors for 3 days. Flow cytometry analysis was performed to measure the expression of HER2 on cell surface within the GFP-positive transfected cells. A HER2-specific antibody conjugated with the Allophycocyanin (APC) fluorophore was used for detection. The numbers represent mean. fluorescence intensity of APC. (E) Cell culture supernatants were harvested from 293FT cells and concentrated. Various dilutions of concentrated supernatants were analysis by Western blotting together with cell lysates. M: protein marker; UB: unboiled; B: boiled. (F) pMX based retroviruses encoding HER2mut or HER2wt were transduced into BT-474 and MCF-7 cells for 6 days prior to AlamarBlue assay. Cells transduced with the control vector pMX. GFP or treated with Herceptin (10 μg/ml) served as negative and positive control, respectively. Percentage cell growth was normalized to that of uninfected control (means ± SEM, n = 6). Double and triple asterisks denote p value < 0.01 and p value < 0.001, respectively. (G) Changes in protein expression were determined in transduced BT-474 cells by Western blotting 3 days post infection. Total HER2 proteins were detected by C-terminus (Abcam) and M45 (Cell signaling) anti-HER2 antibodies, respectively. Phosphorylation of. HER2, ERK and AKT proteins were determined by phospho−specific antibodies. Immunoblotting of β-actin served as protein loading control. C: Control; G: pMX-GFP; mut: HER2mut; wt: HER2wt. (For interpretation of the references to color in this figure legend, the reader is referred to the web version of this article.)

Please cite this article in press as: H. Wang, W. Sun, CRISPR-mediated targeting of *HER2* inhibits cell proliferation through a dominant negative mutation, Cancer Letters (2016), http://dx.doi.org/10.1016/j.canlet.2016.10.033

Cas9 was not due to a reduction in HER2 gene dosage, but was partially attributed to the generation of HER2mut. Our preliminary results revealed that HER2mut lacking the transmembrane domain could be processed for secretion, though the subdomain II of the extracellular domain critical for dimerization was retained [16]. It is plausible that the secreted HER2mut might inhibit the ligand-dependent heterdimerization with other HER receptors. Further investigation is required to determine the exact molecular events involved.

Inhibitors of DNA repair pathways have been exploited for the treatment of human cancers in conjunction with DBSs-inducing chemotherapeutic drugs and ionizing radiation. PARP inhibitors, in particular, appear promising in various cancer types including breast and ovarian cancers [17]. In our study, we showed that Veliparib (PARP1/2 inhibitor) and ME0328 (PARP3 inhibitor) potentiated the targeting efficiency of CRISPR/Cas9 on *HER2*, resulting in a 2–3-fold increased mutation rate. This was accompanied by augmented growth suppression in HER2-positive cells. Therefore, CRISPR/Cas9 in combination with PARP inhibitors could potentially have synergistic anti-cancer effects in the clinical setting. The DNA ligase IV inhibitor SCR7 increased the mutation rate but did not have an inhibitory effect on cell growth. SCR7 might have unspecific activities that interfered with the HER2mut's dominant negative function. Further investigations are required to understand the exact molecular interactions which are beyond the scope of this study.

For therapeutic applications, the potential for off-target effects of the CRISPR/Cas system is a major concern. However, careful design of the guide RNAs as well as subsequent quality checks with whole genome sequencing would reduce the risk of off-target toxicities. There is also a recent report of an engineered CRISPR system that showed improved targeting specificity [18]. Another major issue, as with all other forms of cancer therapy, is the ability of tumors to acquire resistance to the treatment. We believe that the simplicity of the CRISPR system would allow re-targeting of new mutations that underlie resistance by designing new guide RNAs. The relative ease to redirect the Cas9 to target new mutations is a great advantage when compared to the development of conventional therapeutics, which would require initiation of an entirely new drug discovery program.

In summary, we showed that targeting of *HER2* by CRISPR/Cas9 in breast cancer cells resulted in strong anti-tumor activity and the effect can be enhanced by PARP inhibitors treatment. The CRISPR-induced mutations, albeit at low frequencies, produced a truncated HER2 protein exhibiting dominant negative function. The mechanism of action for CRISPR/Cas9 did not appear to involve reduction of HER2 protein expression, but was mediated by a HER2 mutant in a manner different from that of Herceptin. One major hurdle to the translation of the CRISPR/Cas9 system to the clinical setting is in the efficient intracellular delivery of its components. Ideally, all tumor cells must be able to take up the CRISPR/Cas9 components for it to be an effective therapy. Yet, our study suggests that incomplete CRISPR targeting of certain oncogenes within tumors might still have therapeutic value via generation of dominant negative mutations. Future work will make use of the CRISPR system to uncover additional dominant negative alleles and to demonstrate efficacy in xenograft models of cancer.

Acknowledgments

This work was supported by the Institute of Bioengineering and Nanotechnology (Biomedical Research Council, Agency for Science, Technology and Research, Singapore). Q1

The authors wish to thank Motoichi Kurisawa for the provision of Herceptin and Thai LeongYap for helpful discussion and proof-reading of manuscript.

Conflict of interest Q2

The authors declare no potential conflict of interest.

Appendix A. Supplementary data

Supplementary data related to this article can be found at http://dx.doi.org/10.1016/j.canlet.2016.10.033.

References

[1] M.R. Stratton, P.J. Campbell, P.A. Futreal, The cancer genome, Nature 458 (7239) (2009) 719–724.
[2] L. Cong, F.A. Ran, D. Cox, S. Lin, R. Barretto, N. Habib, et al., Multiplex genome engineering using CRISPR/Cas systems, Science 339 (6121) (2013) 819–823.
[3] S.W. Cho, S. Kim, J.M. Kim, J.S. Kim, Targeted genome engineering in human cells with the Cas9 RNA-guided endonuclease, Nat. Biotechnol. 31 (3) (2013) 230–232.
[4] M. Jinek, A. East, A. Cheng, S. Lin, E. Ma, J. Doudna, RNA-programmed genome editing in human cells, eLife 2 (2013) e00471.
[5] P. Mali, L. Yang, K.M. Esvelt, J. Aach, M. Guell, J.E. DiCarlo, et al., RNA-guided human genome engineering via Cas9, Science 339 (6121) (2013) 823–826.
[6] D. Maddalo, E. Manchado, C.P. Concepcion, C. Bonetti, J.A. Vidigal, Y.C. Han, et al., In vivo engineering of oncogenic chromosomal rearrangements with the CRISPR/Cas9 system, Nature 516 (7531) (2014) 423–427.
[7] F.J. Sanchez-Rivera, T. Papagiannakopoulos, R. Romero, T. Tammela, M.R. Bauer, A. Bhutkar, et al., Rapid modelling of cooperating genetic events in cancer through somatic genome editing, Nature 516 (7531) (2014) 428–431.
[8] G. Gasiunas, R. Barrangou, P. Horvath, V. Siksnys, Cas9-crRNA ribonucleoprotein complex mediates specific DNA cleavage for adaptive immunity in bacteria, Proc. Natl. Acad. Sci. U. S. A. 109 (39) (2012) E2579–E2586.
[9] M. Jinek, K. Chylinski, I. Fonfara, M. Hauer, J.A. Doudna, E. Charpentier, A programmable dual-RNA-guided DNA endonuclease in adaptive bacterial immunity, Science 337 (6096) (2012) 816–821.
[10] C. Wyman, R. Kanaar, DNA double-strand break repair: all's well that ends well, Annu. Rev. Genet. 40 (2006) 363–383.
[11] M. Srivastava, S.C. Raghavan, DNA double-strand break repair inhibitors as cancer therapeutics, Chem. Biol. 22 (1) (2015) 17–29.
[12] W.M. Ciszewski, M. Tavecchio, J. Dastych, N.J. Curtin, DNA-PK inhibition by NU7441 sensitizes breast cancer cells to ionizing radiation and doxorubicin, Breast cancer Res. Treat. 143 (1) (2014) 47–55.
[13] M. Srivastava, M. Nambiar, S. Sharma, S.S. Karki, G. Goldsmith, M. Hegde, et al., An inhibitor of nonhomologous end-joining abrogates double-strand break repair and impedes cancer progression, Cell 151 (7) (2012) 1474–1487.
[14] D. Davidson, Y. Wang, R. Aloyz, L. Panasci, The PARP inhibitor ABT-888 synergizes irinotecan treatment of colon cancer cell lines, Investig. New Drugs 31 (2) (2013) 461–468.
[15] A.E. Lindgren, T. Karlberg, A.G. Thorsell, M. Hesse, S. Spjut, T. Ekblad, et al., PARP inhibitor with selectivity toward ADP-ribosyltransferase ARTD3/PARP3, ACS Chem. Biol. 8 (8) (2013) 1698–1703.
[16] M.C. Franklin, K.D. Carey, F.F. Vajdos, D.J. Leahy, A.M. de Vos, M.X. Sliwkowski, Insights into ErbB signaling from the structure of the ErbB2-pertuzumab complex, Cancer Cell 5 (4) (2004) 317–328.
[17] M. Javle, N.J. Curtin, The role of PARP in DNA repair and its therapeutic exploitation, Br. J. Cancer 105 (8) (2011) 1114–1122.
[18] I.M. Slaymaker, L. Gao, B. Zetsche, D.A. Scott, W.X. Yan, F. Zhang, Rationally engineered Cas9 nucleases with improved specificity, Science 351 (6268) (2016) 84–88.

Please cite this article in press as: H. Wang, W. Sun, CRISPR-mediated targeting of *HER2* inhibits cell proliferation through a dominant negative mutation, Cancer Letters (2016), http://dx.doi.org/10.1016/j.canlet.2016.10.033